

# Ferromagnetic resonance of a 2D array of nanomagnets: effects of surface anisotropy and dipolar interactions

J.-L. Déjardin<sup>1,\*</sup>, A. Franco<sup>2,3,†</sup>, F. Vernay<sup>1,‡</sup> and H. Kachkachi<sup>1,§</sup>

<sup>1</sup>Laboratoire PROMES-CNRS (UPR-8521), Université de Perpignan Via Domitia, Rambla de la Thermodynamique, Tecnosud, 66100 Perpignan, FRANCE. and

<sup>2</sup>Departamento de Física, Universidad Técnica Federico Santa María, Avenida España 1680, 2390123 Valparaíso, CHILE

<sup>3</sup>Núcleo de Matemáticas, Física y Estadística, Facultad de Ciencias, Universidad Mayor, Av. Manuel Montt 367, Providencia, Santiago, CHILE

(Dated: June 11, 2018)

We develop an analytical approach for studying the FMR frequency shift due to dipolar interactions and surface effects in two-dimensional arrays of nanomagnets with (effective) uniaxial anisotropy along the magnetic field. For this we build a general formalism on the basis of perturbation theory that applies to dilute assemblies but which goes beyond the point-dipole approximation as it takes account of the size and shape of the nano-elements, in addition to their separation and spatial arrangement. The contribution to the frequency shift due to the shape and size of the nano-elements has been obtained in terms of their aspect ratio, their separation and the lattice geometry. We have also varied the size of the array itself and compared the results with a semi-analytical model and reached an agreement that improves as the size of the array increases. We find that the red-shift of the ferromagnetic resonance due to dipolar interactions decreases for smaller arrays. Surface effects may induce either a blue-shift or a red-shift of the FMR frequency, depending on the crystal and magnetic properties of the nano-elements themselves. In particular, some configurations of the nano-elements assemblies may lead to a full compensation between surface effects and dipole interactions.

## I. INTRODUCTION AND STATEMENT OF THE PROBLEM

Today there are various sophisticated ways of fabricating and characterizing arrays of magnetic nano-elements of tunable magnetic properties that are of interest in practical applications such as magnetic recording, hyperthermia, catalysis and so on. In fundamental and theoretical research, these achievements are welcome as they meet a long-standing demand for well-defined structures with controllable parameters such as the size, the shape and spatial organization. On the other hand, experimental techniques of characterization and measurements have known great progress with regards to spatial and temporal resolution, thus further bridging the gap between the nanometer and macroscopic scales. Ferromagnetic resonance (FMR)<sup>1-8</sup> is one of such very precise techniques that has been upgraded to detect the resonance of small arrays of nanocubes with a sensitivity of  $10^6 \mu_B$ . Other variants of the FMR spectroscopy, such as the so-called Magnetic Resonance Force Microscopy (MRFM)<sup>9</sup> may be used for the characterization of cobalt nano-spheres<sup>10</sup>. Standard FMR theory<sup>11</sup>, based on microwave absorption in magnetic materials, shows that the resonance frequency is, to a first approximation, a function of the effective field which usually comprises the magneto-crystalline and shape anisotropy, the exchange coupling and the applied (static) magnetic field. This dependence can be used to characterize the material's parameters. On the other hand, these parameters can be varied so as to control the microwave absorption properties of the material. For instance, the dipolar interac-

tions (DI) between nano-elements can be modulated by the elements density. A dipolar coupling between (parallel) elongated objects induces an additional anisotropy with an easy axis along the DI bond and perpendicular to the objects. In Refs. 12,13 it was shown that the direction of the effective anisotropy can be tuned parallel or perpendicular to the nano-elements axes by varying the concentration. This two-way relationship between the FMR characteristics and the system's physical parameters is usually based on analytical expressions that provide the resonance frequency as a function of the material's parameters (anisotropy constants, exchange and dipolar couplings). In the case of an array of interacting magnetic nano-elements such analytical expressions cannot be obtained in a closed form and one has to resort to some approximation, *e.g.* that of weak interactions (which can experimentally be tuned, for instance, for core-shell nanoparticles<sup>14</sup>), or equivalently of dilute assemblies. Accordingly, one can apply perturbation theory and derive approximate expressions for the resonance frequency of the interacting assembly, taking into account the size and form of both the nano-elements and the array, in addition to the (effective) anisotropy and applied DC field. As the size decreases surface effects (SE) start to play a critical role in the magnetic properties of the nanomagnets, especially in monodisperse assemblies with oriented effective anisotropy. For ratios of the surface anisotropy constant  $K_s$  to the exchange coupling  $J$  smaller than unity ( $K_s/J < 1$ )<sup>15-17</sup>, the spin configuration within the nano-magnet may be considered as quasi-collinear<sup>18,19</sup>. Then, an effective model for the (macroscopic) net magnetic moment of the nano-magnet can be built and which properly accounts for the magnetic prop-

erties (static and dynamical) of the nano-magnet<sup>18–21</sup>. Using this model, we extend our analytical study by including the effects of both dipolar interactions and surface anisotropy and their competition [see Section III]. Therefore, the main objective of the present work is to i) derive the correction to the resonance frequency due to DI using perturbation theory, beyond the point-dipole approximation, *i.e.* taking account of the shape and size of the nano-elements (or dipoles) and ii) derive the shift of the resonance frequency due to surface effects using the effective model for each nano-element<sup>18,19</sup>. Then, we apply this formalism to the prototypical case of an array of thin disks and derive the corresponding approximate expression for the frequency shift induced by DI. Next, we analyze the contribution from surface anisotropy to the FMR frequency and compare with the DI-induced shift.

Another general approach has been developed in Ref. 22 for studying the collective dipolar (or magnonic) spin-wave excitations in a two dimensional array of magnetic nano-dots, in the absence of magneto-crystalline anisotropy. Other similar works and approaches can be found in the literature<sup>23–25</sup> which deal with collective effects in assemblies of nano-elements. In the present work we adopt a general but simple approach that allows us to take into account surface effects as well as dipolar interactions and to study their competition, in dilute and monodisperse assemblies with oriented magneto-crystalline (effective) uniaxial anisotropy. Moreover, for practical reasons related with the possibility to compare with experiments, we focus on FMR resonance and provide explicit analytical expressions for the frequency shift induced by dipolar interactions and surface anisotropy. As was discussed above, today several experimental groups<sup>5,6,8,10,23–30</sup> are able to fabricate well organized and almost monodisperse assemblies of cobalt or iron-oxide nano-particles and aim at measuring their ferromagnetic resonance frequency and resonance field. It is then desirable to have at least approximate but simple analytical formulas to compare with the experimental results and to infer rough estimates of the most relevant physical parameters, such as the elements size and separation.

This paper has been organized as follows. In Section I, we define the system and its energy, focusing on the contribution from the dipolar interactions. In Section II we present our general formalism in a matrix form and derive the final expression for the frequency shift due to DI. Next, this formalism is applied to a 2D array of nano-magnets and explicit expressions are then given for the various contributions to the energy and for the frequency shift, in particular in the case of thin disks. We also discuss the contribution that stems from the size and shape of the nano-elements, which adds up to the contribution that obtains within the point-dipole approximation. In Section III we present the effective model for angular isolated nano-element and discuss the surface contribution to the frequency shift. Section IV shows some re-

sults of the comparison between the numerical and semi-analytical calculations of the frequency shift. We also discuss the effect of the array size on the difference in frequency shift between the results of the two approaches. Finally, we discuss the competition between DI and surface effects in two situations with a positive or negative contribution from the latter. The paper ends with our conclusions and two short appendices.

## A. Energy

Here we define the systems targeted by this study and discuss the various contributions to their energy, with a special focus on the dipolar interactions. For simplicity, the discussion of the contribution to the energy from the nano-element surface anisotropy is postponed to Section III.

Consider a monodisperse array of magnetic nano-elements each (of volume  $V$ ) carrying a magnetic moment  $\mathbf{m}_i = m_i \mathbf{s}_i$ ,  $i = 1, \dots, \mathcal{N}$  of magnitude  $m_i = M_s V$  and direction  $\mathbf{s}_i$ , with  $|\mathbf{s}_i| = 1$ ,  $M_s$  being the saturation magnetization. The energy (in S.I. units) of the magnetic moment  $\mathbf{m}_i$  is given by

$$E_i = E_i^{(0)} + E_{\text{DI},i}, \quad (1)$$

where  $E_i^{(0)}$  is the energy of the non-interacting nano-elements that comprises the Zeeman and (effective) anisotropy energies, and the second term  $E_{\text{DI}}$  is the DI contribution. The total energy of the system is  $E = \sum_{i=1}^{\mathcal{N}} E_i$ .

For two magnetic nano-elements carrying macroscopic moments  $\mathbf{m}_i$  and  $\mathbf{m}_j$ , located at two arbitrary sites  $i$  and  $j$ , the dipolar interaction reads (in SI units)

$$E_{\text{DI},i,j} \equiv \left( \frac{\mu_0}{4\pi} \right) \mathbf{m}_i \cdot \mathcal{D}_{ij} \cdot \mathbf{m}_j \quad (2)$$

where  $\mathcal{D}_{ij}$  is the corresponding tensor [see Eq. (12)]. Summing over all pair-wise interactions, avoiding double counting, yields the energy of a magnetic moment at site  $i$  due to its interaction with all other moments in the assembly with the corresponding energy

$$E_{\text{DI},i} \equiv \left( \frac{\mu_0}{4\pi} \right) \sum_{j < i} \mathbf{m}_i \cdot \mathcal{D}_{ij} \cdot \mathbf{m}_j. \quad (3)$$

If one denotes by  $R_{ij}$  the distance between the sites  $i$  and  $j$  and use  $\mathbf{m}_i = m_i \mathbf{s}_i$ ,  $\mathbf{m}_j = m_j \mathbf{s}_j$ , we see that  $E_{\text{DI},i}$  scales as  $m^2/R^3$ . Next, we may introduce the distance  $d$  as the nearest-neighbor inter-particle separation, or the “super-lattice” parameter, and write  $R_{ij} = r_{ij}d$  where now  $r_{ij}$  is a dimensionless parameter, which is calculated as usual using only the integer indices used to locate a site on a given lattice. More precisely, a site  $i$  on discrete 2D lattice, for instance, can be located using its coordinates  $x_i, y_i \in \mathbb{R}$  or by the corresponding integer indices

$i_x, i_y \in \mathbb{N}$ . Then,  $R_{ij} = \sqrt{(x_i - x_j)^2 + (y_i - y_j)^2}$  while  $r_{ij} = \sqrt{(i_x - j_x)^2 + (i_y - j_y)^2} = R_{ij}/d$ . Therefore, when dealing with DI on a super-lattice, it is quite natural to introduce the parameter

$$\lambda \equiv \left(\frac{\mu_0}{4\pi}\right) \frac{m^2}{d^3}, \quad (4)$$

to characterize the strength of the DI in the system since the dipolar energy in Eq. (2) scales with  $\lambda$ .

In the next section, we will apply our formalism to specific situations where the expressions of all contributions to the energy can be explicitly written.

In the present work, we develop a general formalism that can be applied to an arbitrary system of interacting arrays of nano-magnets. However, here it will be applied to the specific case of a two-dimensional mono-disperse array of nano-magnets, with the main objective to derive explicit expressions for the FMR frequency shift induced by the DI and SE. These calculations are based on perturbation theory for a dilute assembly but are valid for nano-magnets of arbitrary size and shape, thus going beyond the simple point-dipole approximation (PDA). On other hand, in Section III we discuss in detail surface effects that come into play when the size of the nano-elements becomes small enough (with the number of surface atoms exceeding 50%). In the framework of the effective model discussed earlier, we will discuss how the expressions in the present section are extended to include the contribution from surface anisotropy.

To summarize, our simplification only refer to: *i*) a collective condition which assumes that the assembly is diluted. That is to say the center-to-center distance between the nanoelements is much larger than the linear dimension of the nanoelements. *ii*) An intrinsic condition requiring that the magnetic state of the nanoelements is nearly saturated by the applied magnetic field. Now, the geometry of the nanoelements themselves or that of the sample (*i.e.* the assembly thereof) are brought in by the dipolar tensor  $\mathcal{D}$  and the distribution of the distances  $r_{ij}$ .

Therefore, we consider a 2D array of magnetic nano-elements which we assume to be lying in the  $yz$  plane, for mathematical convenience. The applied magnetic field and the (magneto-crystalline) uniaxial anisotropy easy axes  $\mathbf{e}_i$  are all directed along the  $x$  axis, *i.e.*  $\mathbf{H} = H\mathbf{e}_x$  and  $\mathbf{e}_i = \mathbf{e}_x$  for all  $i = 1, \dots, \mathcal{N}$ . As shown in Fig. 1, we adopt the usual spherical coordinates for the magnetization orientation

$$\mathbf{s}_i = \begin{cases} s_{ix} = \sin \theta_i \cos \varphi_i & = s_i^\perp \cos \varphi_i, \\ s_{iy} = \sin \theta_i \sin \varphi_i & = s_i^\perp \sin \varphi_i, \\ s_{iz} = \cos \theta_i & = \cos \theta_i, \end{cases} \quad (5)$$

with  $|\mathbf{s}_i| = 1$ .

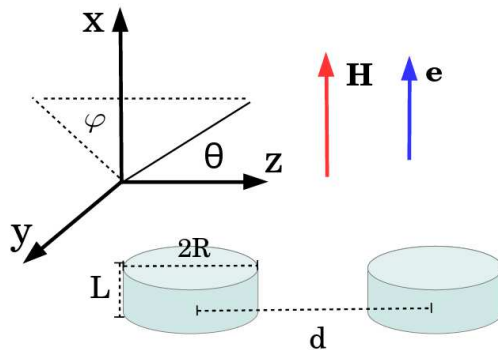


Figure 1: A pair of magnetic nano-elements belonging to the 2D array (in the  $yz$  plane), of diameter  $D = 2R$ , height  $L$  and separation  $d$ . The standard system of spherical coordinates  $(\theta, \varphi)$  is also shown together with the setup of the magnetic field  $\mathbf{H}$  and (magneto-crystalline) anisotropy easy axes  $\mathbf{e}$ .

In Eq. (1) the energy density  $E_i^{(0)}$  of an isolated nano-element (ignoring its SE) is given by

$$E_i^{(0)} = -\mu_0 M_s \mathbf{H} \cdot \mathbf{s}_i - K_2 (\mathbf{s}_i \cdot \mathbf{e}_i)^2 + E_{\text{demag}} \quad (6)$$

where  $K_2$  is the magneto-crystalline (uniaxial) anisotropy constant,  $\mathbf{e}_i$  the uniaxial anisotropy easy axis directed along the  $x$  axis (see Fig. 1). The term  $E_{\text{demag}}$  in Eq. (6) is the magnetostatic energy density

$$E_{\text{demag}} = -\frac{\mu_0}{2} M_s \mathbf{H}_d \cdot \mathbf{s}_i = \frac{\mu_0}{2} M_s^2 \mathbf{s}_i \mathbf{N} \cdot \mathbf{s}_i \quad (7)$$

where  $\mathbf{N}$  is the demagnetization tensor and  $\mathbf{H}_d$  the demagnetizing field.

A rigorous evaluation of the demagnetization tensor for uniformly magnetized particles with cylindrical symmetry was provided in Refs. [31] using elliptical integrals [see Eq. (74) therein]. However, as already emphasized earlier, our goal here is to derive an approximate analytical expression for the FMR frequency shift due to DI. Now, FMR measurements are performed under a DC magnetic field that is strong enough for saturating the magnetic system, and this leads to a smoothing out of the spin non-colinearities that usually occur in a magnetic system, especially when its aspect ratio differs from unity. In addition, in our system setup, the external magnetic field is applied in the direction of uniaxial anisotropy, thus leading to a strong effective field along the cylinder axis. In such a situation, the calculations of the demagnetizing field greatly simplify, as is exemplified by Eqs. (26) and (27) of Ref. [32]. Consequently, after averaging over the sample's length, the following approximate expression for the demagnetization factors for a nano-element with cylindrical symmetry about the  $x$  axis (as is the case here) is obtained<sup>33</sup>

$$N_x = (1 + \delta) - \sqrt{1 + \delta^2}, \\ N_y = N_z = \frac{1}{2} \left( \sqrt{1 + \delta^2} - \delta \right),$$

where  $\delta \equiv R/L$ , with  $R$  being the radius of the cylinder and  $L$  its length (or thickness). In particular, for a very long cylinder with  $R \ll L$  ( $\delta \ll 1$ ), the longitudinal demagnetization factor  $N_x \rightarrow 0$  while the transverse factors  $N_z = N_y \rightarrow 1/2$ . In the opposite limit, for a very thin disk,  $R \gg L$  ( $\delta \gg 1$ ),  $N_x \rightarrow 1$  and  $N_z = N_y \rightarrow 0$ .

Therefore, using  $|\mathbf{s}_i| = 1$  the demagnetizing energy density becomes (up to a constant)

$$E_{\text{demag}} = \frac{\mu_0}{2} M_s^2 (N_x - N_z) s_{i,x}^2. \quad (8)$$

The effective field  $\mathbf{H}_{\text{eff},i} = -\frac{1}{M_s} \delta E_i^{(0)} / \delta \mathbf{s}_i$ , normalized with respect to the anisotropy field

$$\mu_0 H_K = \frac{2K_2}{M_s}, \quad (9)$$

namely  $\mathbf{H}_{\text{eff},i} \rightarrow \mathbf{h}_{\text{eff},i} \equiv \mathbf{H}_{\text{eff},i} / H_K$ , and upon dropping the index  $i$  (for simplicity), reads

$$\mathbf{h}_{\text{eff}} = [h + k s_x + h_d s_x] \mathbf{e}_x \quad (10)$$

where  $h \equiv H/H_K$ ,  $h_d \equiv -\mu_0 M_s (N_x - N_z) / H_K$  and  $k$  ( $= 0$  or  $1$ ) is a label merely introduced for keeping track of the contribution from magneto-crystalline anisotropy.

The angular frequency of an isolated nano-element is given by  $\omega^{(0)} = \gamma H_{\text{eff}}$ , with  $\gamma \simeq 1.76 \times 10^{11}$  (T.s) $^{-1}$  being the gyromagnetic ratio. Since, in the present setup, the minimum-energy state of the nano-magnet corresponds to having its magnetic moment along the  $x$  axis, we have  $\omega^{(0)} = \omega_K (h + k + h_d)$ , where  $\omega_K \equiv \gamma H_K$ . Thus, for convenience we also introduce the dimensionless angular frequency

$$\varpi^{(0)} \equiv \frac{\omega^{(0)}}{\omega_K} = h + k + h_d \quad (11)$$

In the sequel, we shall measure all frequencies in units of  $\omega_K$ , *i.e.*,  $\varpi \equiv \omega / \omega_K$ .

## B. Dipolar interactions beyond the point-dipole approximation

For a pair of magnetic nano-elements belonging to the  $2D$  array, as shown in Fig. 1, the DI interaction was obtained in this horizontal configuration in Ref. 34, see also Ref. 23. It is given by

$$\mathcal{E}_{\text{DI}} \equiv \frac{E_{\text{DI}}}{2K_2 V} = \frac{1}{2} \sum_{i=1}^{\mathcal{N}} \sum_{\substack{j=1 \\ j \neq i}}^{\mathcal{N}} \xi_{ij} \mathbf{s}_i \cdot \mathcal{D}_{ij} \mathbf{s}_j \quad (12)$$

where

$$\mathcal{D}_{ij} = \frac{J_{ij} - (2 + \Phi_{ij}) \hat{\mathbf{r}}_{ij} \hat{\mathbf{r}}_{ij}}{r_{ij}^3}$$

is the usual DI dyadic and  $\hat{\mathbf{r}}_{ij}$  the unit vector connecting the sites  $i$  and  $j$ , *i.e.*  $\hat{\mathbf{r}}_{ij} = \mathbf{r}_{ij} / r_{ij}$ .  $J_{ij}$  is the diagonal matrix

$$J_{ij} = \begin{pmatrix} \Phi_{ij} & 0 & 0 \\ 0 & 1 & 0 \\ 0 & 0 & 1 \end{pmatrix}$$

and  $\Phi_{ij}$  is a function of the size and shape of the nano-elements as well as their separation [see Fig. 1 (right)]. It is defined by<sup>23,34</sup>

$$\Phi_{ij}(\eta_{ij}, \tau) \equiv \frac{\mathcal{I}_d^h(\eta_{ij}, \tau)}{\mathcal{I}_d^h(\eta_{ij}, \tau)} \quad (13)$$

with

$$\begin{aligned} \mathcal{I}_d^h(\eta, \tau) &= 16\eta^2 \tau \int_0^\infty \frac{dq}{q^2} J_1^2(q) J_1(2\eta\tau q) \left[ 1 - \frac{(1 - e^{-2q\tau})}{2q\tau} \right], \\ \mathcal{J}_d^h(\eta, \tau) &= 16\eta^3 \tau \int_0^\infty \frac{dq}{q^2} J_1^2(q) J_0(2\eta\tau q) (1 - e^{-2\tau q}). \end{aligned} \quad (14)$$

$J_0$  and  $J_1$  are the well known Bessel functions. We have also introduced the following geometrical or ‘‘aspect-ratio’’ parameters

$$\eta_{ij} \equiv \frac{r_{ij} d}{L}, \tau \equiv \frac{L}{2R}. \quad (15)$$

Note that  $r_{ij} d$  is the center-to-center distance between the pair of nano-elements on sites  $i, j$ , with  $d$  being the (super-lattice) step of the array ( $r_{ij}$  are dimensionless real numbers). Finally, the DI coefficient  $\xi_{ij}$ , appearing in Eq. (12), is given by [see Eq. (4)]

$$\xi_{ij} \equiv \frac{\lambda}{2K_2 V} \mathcal{I}_d^h(\eta_{ij}, \tau). \quad (16)$$

Now, we discuss the equilibrium state of the system. In general this is obtained by minimizing the total energy of the system with respect to all degrees of freedom. In the present case, we would have to minimize the energy (1), summed over the whole lattice, with respect to the  $2\mathcal{N}$  angles  $\theta_i, \varphi_i, i = 1, \dots, \mathcal{N}$ . In general, it is well known to the numerical-computing community that minimization of such a multi-variate function is a formidable task that requires a lot of efforts and high computing powers. Apart from the latter, one of the reasons is that there are no ‘‘automatic’’ algorithms for finding the absolute minimum of the function and for each situation, one has to guide the solver through some prescribed path(s). Since the interactions are pair-wise, one could also proceed by obtaining the energy minima for a dimer and then sum over the lattice. The equilibrium state of a dimer with DI in several configurations of anisotropy and applied field were thoroughly studied in Ref. 34 and the various extrema were found in a closed form. However, it is clear

that for interactions of arbitrary intensity the state of an  $(N + 1)$ -body system does not necessarily include the state of the  $N$ -body system. For this reason the states obtained in Ref. 34 cannot just be extended to the array studied here by summing over the lattice index. As such, and as stated earlier, we resort to an analytical treatment based on a few simplifying assumptions. Accordingly, we first assume that the DI are weak enough as to allow for such an extension. In fact, in FMR measurements, the applied magnetic field is usually strong enough as to saturate the magnetic state of the system, and this leads to the nearly linear branch of the resonance frequency as a function of the amplitude of the applied field. This is the situation that we adopt here. Usually the DI in such a 2D array (oblate assembly) favor a net magnetic moment in the plane of the array. However, the strong effective anisotropy and the (relatively) strong magnetic field are parallel to each other and perpendicular to the array's plane, and should then lead to a reorientation of all magnetic moments towards their direction. For this reason, the setup in Fig. 1 leads to the equilibrium state:  $\theta_i = \frac{\pi}{2}$ ,  $\varphi_i = 0$ ,  $i = 1, \dots, \mathcal{N}$ .

The effect of dipolar interactions in ordered and disordered low-dimensional nanoparticle assemblies have been studied by many authors<sup>35</sup>. In dense assemblies, the DI lead to various local magnetic orders that depend on the lattice structure<sup>35,36</sup>. Under some conditions, they may also induce long-range order leading to the so-called super-ferromagnetic state<sup>28</sup>. Obviously, the situation we consider here is quite different in that the concentration we assume is not high enough as to lead to the onset of assembly-wide collective states. In addition, as argued earlier we assume that the DI do not modify the equilibrium state as determined by a competition between the applied field and the anisotropy. However, even such a weak intensity of DI would be important to the dynamics of the assembly since then the energy barriers and thereby the relaxation rates would be affected.

## II. FMR SPECTRUM : GENERAL FORMALISM

In this section, we present the general formalism we have developed in order to derive approximate analytical expressions for the shift of the FMR frequency induced by dipolar interactions.

### A. Landau-Lifshitz equation and FMR eigenvalue problem

The time evolution of the magnetization orientation  $\mathbf{s}_i$  is governed by the damped (norm-conserving) Landau-Lifshitz equation (LLE)

$$\frac{d\mathbf{s}_i}{dt_r} = -\mathbf{s}_i \times \mathbf{h}_{\text{eff},i} + \alpha \mathbf{s}_i \times (\mathbf{s}_i \times \mathbf{h}_{\text{eff},i}), \quad (17)$$

where  $\mathbf{h}_{\text{eff},i}$  now comprises both the free and interacting parts of the system's energy.  $\alpha$  ( $\lesssim 1$ ) the phenomenological damping parameter and  $t_r$  is the (dimensionless) time defined by  $t_r = t/t_s$ , where  $t_s = \omega_K^{-1}$  is the nanoelement's characteristic timescale.

In order to compute the spectrum of the system excitations we may proceed by linearizing the LLE (17) about the equilibrium state. Indeed, we assume that the equilibrium state, which minimizes the system's energy, denoted by  $\{\mathbf{s}_i^{(0)}\}_{i=1,\dots,\mathcal{N}}$ , has been determined with the help of some analytical or numerical technique. Then, we may write  $\mathbf{s}_i \simeq \mathbf{s}_i^{(0)} + \delta\mathbf{s}_i$  and transform the differential equation (17) into the following equation<sup>37</sup>

$$\frac{d(\delta\mathbf{s}_i)}{dt_r} = \sum_{k=1}^{\mathcal{N}} [\mathcal{H}_{ik}\mathcal{I}(\alpha)] \delta\mathbf{s}_k, \quad i = 1, \dots, \mathcal{N} \quad (18)$$

with the (pseudo-)Hessian

$$\mathcal{H}_{ik}[\mathcal{E}] \equiv \begin{pmatrix} \partial_{\theta_k\theta_i}^2 \mathcal{E} & \frac{1}{\sin\theta_i} \partial_{\theta_k\varphi_i}^2 \mathcal{E} \\ \frac{1}{\sin\theta_k} \partial_{\varphi_k\theta_i}^2 \mathcal{E} & \frac{1}{\sin\theta_k \sin\theta_i} \partial_{\varphi_k\varphi_i}^2 \mathcal{E} \end{pmatrix} \quad (19)$$

whose matrix elements are second-order derivatives of the energy with respect to the spherical angles of  $(\theta_i, \varphi_i)$  that determine the direction  $\mathbf{s}_i$ . All these matrix elements are evaluated at the equilibrium state  $\{\mathbf{s}_i^{(0)}\}_{i=1,\dots,\mathcal{N}}$ . The symbol  $\partial_{\alpha_k\beta_i}^2$  stands for the second derivative with respect to the angles  $\alpha_k, \beta_i$ .

The matrix

$$\mathcal{I}(\alpha) \equiv \begin{pmatrix} \alpha & -1 \\ 1 & \alpha \end{pmatrix}$$

stems from the double cross product in Eq. (17).

Next, one may seek solutions of Eq. (18) in the form  $\delta\mathbf{s}_k = \delta\mathbf{s}_k(0) e^{i\Omega\tau}$  leading to the following eigenvalue problem

$$\sum_{k=1}^{\mathcal{N}} [\mathcal{H}_{ik}\mathcal{I}(\alpha) - i\Omega\mathbb{1}] \delta\mathbf{s}_k = 0 \quad (20)$$

whose set of roots  $\{\Omega_n\}_{1 \leq n \leq \mathcal{N}}$  yields the system's eigenfrequencies,  $f_n = -i\frac{\Omega_n}{2\pi} = \frac{\omega_n}{2\pi}$ , where  $\omega_n$  is the real angular frequency (in rad/s). Here,  $\mathbb{1}$  is the identity matrix with matrix elements  $\mathbb{1}_{ik}^{\mu\nu} = \delta_{ik}\delta^{\mu\nu}$ .

In the general case of an array of nano-elements with arbitrary DI, it is not possible to determine the system's exact equilibrium state  $\{\mathbf{s}_i^{(0)}\}_{i=1,\dots,\mathcal{N}}$  that minimizes the total energy of the system, including the (core and surface) anisotropy, the DI and the applied field. In addition, it is not an easy matter to solve the eigenvalue problem (20) in its full generality. Of course, these tasks can be numerically accomplished to some extent. However, as stated earlier, our objective here is to obtain an analytical expression for the FMR frequency. In order to

do so, we restrict ourselves to the case of dilute assemblies of nanomagnets, and as such, we solve the eigenvalue problem (20) using perturbation theory that we present now.

### B. DI correction to FMR frequency : perturbation theory

In the following we only consider the undamped case, *i.e.* with  $\alpha = 0$  [see Eq. (17)], we present our formalism in the general case.

As we have seen, the excitation spectrum can be obtained by diagonalizing the matrix  $\mathbb{H}_{ik}(\alpha) \equiv \mathcal{H}_{ik}\mathcal{I}(\alpha)$  of matrix elements

$$\mathbb{H}_{ik}^{\mu\nu}(\alpha) = \sum_{\rho=\theta,\varphi} \mathcal{H}_{ik}^{\mu\rho}\mathcal{I}^{\rho\nu}(\alpha).$$

A word is in order regarding the various indices. The problem being studied here is an array of magnetic moments located at the nodes of a super-lattice. Hence, there are two kinds of indices. The first one, using the Greek letters  $\mu, \nu, \rho$ , refers to the components of a magnetic moment in the system of spherical coordinates and thus assumes the values  $\theta, \varphi$ . The second index, using the Roman letters  $i, j, k$ , refers to the lattice site and assumes the values  $1, \dots, \mathcal{N}$ . Therefore, the full “phase space” is a direct product of the two sub-spaces corresponding to the two kinds of variables. Likewise, the matrices involved in these calculations are tensor products of the corresponding sub-matrices.

If we focus on dilute assemblies with relatively weak DI we can write the total energy as the sum of the energy of the non-interacting assembly and the interaction contribution, *i.e.*  $\mathcal{E} = \mathcal{E}^{(0)} + \mathcal{E}_{\text{DI}}$ , with  $\mathcal{E} \equiv E/(2K_2V)$  and similarly for each contribution. Then, the pseudo-Hessian  $\mathcal{H}_{ik}(\mathcal{E}_i)$  can also be correspondingly split as follows

$$\mathbb{H}_{ik}^{\mu\nu}(\alpha) = \mathcal{F}_{ik}^{\mu\nu} + \Xi_{ik}^{\mu\nu} \quad (21)$$

where  $\mathcal{F}_{ik}$  is the contribution in the absence of interactions given by the same matrix as in Eq. (19), upon substituting  $\mathcal{E}^{(0)}$  for  $\mathcal{E}$ , and multiplied by  $\mathcal{I}(\alpha)$ . Thus,  $\mathcal{F} = \mathcal{H}[\mathcal{E}^{(0)}]\mathcal{I}(\alpha)$ . Similarly,  $\Xi_{ik}$  is the DI contribution given by the matrix in Eq. (19), with substitution of  $\mathcal{E}_{\text{DI}}$  for  $\mathcal{E}$ , multiplied by  $\mathcal{I}(\alpha)$ , *i.e.*  $\Xi = \mathcal{H}[\mathcal{E}_{\text{DI}}]\mathcal{I}(\alpha)$ . For later use, we introduce the two matrices  $F \equiv \mathcal{H}[\mathcal{E}^{(0)}]$ ,  $\Theta \equiv \mathcal{H}[\mathcal{E}_{\text{DI}}]$ .

It is understood that wherever they appear all matrix elements have to be evaluated at the equilibrium state  $\{\mathbf{s}_i^{(0)}\}_{i=1,\dots,\mathcal{N}}$  with  $\mathbf{s}_i^{(0)} = (1, 0, 0)$ . In the situation of relatively weak coupling considered here, we make the

further assumption that the equilibrium state is not altered by the dipolar interactions. More precisely, we assume that the main equilibrium of the system is setup by the competition between the strong (effective) anisotropy and the external DC magnetic field. Of course, the DI of arbitrary strength would change both the energy minima and saddle points of the system, and thereby significantly change its dynamics. Here we restrict ourselves to the situation where the DI only contribute through the second term in Eq. (21), which is regarded as a correction to the first term. This assumption is experimentally relevant for dilute assemblies. For instance, it has been demonstrated<sup>14</sup> that inter-particle interactions in assemblies of core-shell ( $\text{Fe}_3\text{O}_4/\text{SiO}_2$ ) nanoparticles can be tuned by modifying the thickness of the shell.

Therefore, in spin components the LLE (18) reads

$$\frac{d(\delta s_i^\mu)}{dt} = \sum_{\nu=\theta,\varphi} \sum_{k=1}^{\mathcal{N}} [\mathcal{F}(\mathbb{1} + \mathcal{F}^{-1}\Xi)]_{ik}^{\mu\nu} \delta s_k^\nu. \quad (22)$$

Regarding the various indices discussed above, the matrix  $\mathcal{F}$  of the non-interacting array can be written as  $\mathcal{F} = \mathcal{F}_{2 \times 2} \otimes \mathbb{1}_{\mathcal{N} \times \mathcal{N}}$ , or in components  $\mathcal{F}_{ik}^{\mu\nu} = (\mathcal{F}_{2 \times 2}^{\mu\nu})_i \delta_{ik} = \delta_{ik} \mathcal{H}[\mathcal{E}^{(0)}]_{ii}^{\mu\nu} \mathcal{I}(\alpha)$ . Using the matrix  $F$  introduced earlier, the matrix  $\mathcal{F}$  explicitly reads

$$\mathcal{F}_{ik} = \delta_{ik} \begin{pmatrix} F_{ii}^{\theta\varphi} & -F_{ii}^{\theta\theta} \\ F_{ii}^{\varphi\varphi} & -F_{ii}^{\varphi\theta} \end{pmatrix} \otimes \mathbb{1}.$$

Note that the  $2 \times 2$  matrix above has two eigenvalues  $\pm i\varpi_i^{(0)}$ , where  $\varpi_i^{(0)}$  is the (normalized) resonance frequency of the magnetic moment at site  $i$  in the non-interacting case. In fact, for the mono-disperse assemblies considered here all these frequencies are identical, *i.e.*  $\varpi_i^{(0)} \equiv \varpi^{(0)}$ , defined in Eq. (11). Hence,  $\det \mathcal{F} = \prod_i^{\mathcal{N}} (\varpi_i^{(0)})^2 = (\varpi^{(0)})^{2\mathcal{N}}$ .

On the other hand, the matrix  $\Xi$  introduced above and which contains the DI contribution can also be written explicitly to some limit. Again, using the matrix  $\Theta$  introduced earlier, the  $2 \times 2$  diagonal block of the matrix  $\Xi = \mathcal{H}[\mathcal{E}_{\text{DI}}]\mathcal{I}(\alpha)$  reads

$$\begin{pmatrix} \Theta_{ii}^{\theta\varphi} & -\Theta_{ii}^{\theta\theta} \\ \Theta_{ii}^{\varphi\varphi} & -\Theta_{ii}^{\varphi\theta} \end{pmatrix}, \quad i = 1, 2, \dots, \mathcal{N}. \quad (23)$$

One should note that these DI matrix elements with identical lattice sites are not equal to zero even if they correspond to pair-wise interactions. Indeed, in the most general situation, the second derivatives of the energy are given by

$$\begin{aligned}
\partial_{\theta_i \theta_k}^2 \mathcal{E} &= \delta_{ik} [\mathbf{s}_i \cdot -\mathbf{e}_{\theta_i} \cdot (\mathbf{e}_{\theta_i} \cdot \nabla_i)] \mathbf{h}_{\text{eff},i} - (1 - \delta_{ik}) \mathbf{e}_{\theta_i} \cdot [\mathbf{e}_{\theta_k} \cdot \nabla_k] \mathbf{h}_{\text{eff},i}, \\
\partial_{\varphi_k \varphi_i}^2 \mathcal{E} &= \delta_{ik} \sin \theta_i [(\sin \theta_i \mathbf{s}_i + \cos \theta_i \mathbf{e}_{\theta_i}) - \sin \theta_i \mathbf{e}_{\varphi_i} \cdot (\mathbf{e}_{\varphi_i} \cdot \nabla_i)] \mathbf{h}_{\text{eff},i} - (1 - \delta_{ik}) \sin \theta_i \sin \theta_k \mathbf{e}_{\varphi_i} \cdot [\mathbf{e}_{\varphi_k} \cdot \nabla_k] \mathbf{h}_{\text{eff},i}, \\
\partial_{\theta_k \varphi_i}^2 \mathcal{E} &= -\delta_{ik} [\cos \theta_i \mathbf{e}_{\varphi_i} \cdot + \sin \theta_i \mathbf{e}_{\varphi_i} \cdot (\mathbf{e}_{\theta_i} \cdot \nabla_i)] \mathbf{h}_{\text{eff},i} - (1 - \delta_{ik}) \sin \theta_i \mathbf{e}_{\varphi_i} \cdot [\mathbf{e}_{\theta_k} \cdot \nabla_k] \mathbf{h}_{\text{eff},i}, \\
\partial_{\varphi_k \theta_i}^2 \mathcal{E} &= -\delta_{ik} [\cos \theta_i \mathbf{e}_{\varphi_i} \cdot + \sin \theta_i \mathbf{e}_{\theta_i} \cdot [\mathbf{e}_{\varphi_i} \cdot \nabla_i]] \mathbf{h}_{\text{eff},i} - (1 - \delta_{ik}) \sin \theta_k \mathbf{e}_{\theta_i} \cdot (\mathbf{e}_{\varphi_k} \cdot \nabla_k) \mathbf{h}_{\text{eff},i}.
\end{aligned} \tag{24}$$

Explicit expressions for the DI energy only are given in Appendix A. Note then that because of the first term in each line of Eq. (24), the second derivatives  $\Theta_{ii}^{\mu\nu}$  do not vanish even for the DI contribution, and using (19, A1) we do see that  $\Theta_{ii}^{\mu\nu} \neq 0$ . However, we stress that the DI contribution to  $\mathbf{h}_{\text{eff},i}$  contains a sum over the whole lattice except (for the site  $i$ ) and thus the DI coefficient entering  $\mathbf{h}_{\text{eff},i}$  involves a sum over  $j$  with  $j \neq i$ . Obviously, the matrix  $\Xi$  has also nonzero off-diagonal blocks which are of the same form as in (23) but with distinct indices  $i, k = 1, 2, \dots, \mathcal{N}$ , *i.e.*  $i \neq k$ .

Now, we introduce the new tensor  $\Lambda \equiv \mathcal{F} (\mathbf{1} + \mathcal{F}^{-1} \Xi)$

$$\det \Lambda = \det \mathcal{F} \times \det (\mathbf{1} + \mathcal{F}^{-1} \Xi). \tag{25}$$

and set to compute its determinant. Similarly to  $\varpi_n^{(0)}$  (the eigenvalues of  $\mathcal{F}$ ) we introduce the eigenvalues  $\varpi_n$  as the resonance frequencies with the index  $n$  running through all the  $2\mathcal{N}$  (collective) modes of the interacting system. This leads to  $\det \Lambda = \prod_{n=1}^{\mathcal{N}} \varpi_n^2$ . Then, let us examine the last determinant in Eq. (25). The product  $\mathcal{F}^{-1} \Xi$  scales with the ratio  $\lambda/H$ , *i.e.* the ratio of the DI intensity  $\lambda = (\frac{\mu_0}{4\pi}) m^2/d^3$  to the static magnetic field  $H$ . This ratio is obviously small for a dilute assembly, especially for standard FMR measurements where the DC field is usually taken strong enough to saturate the sample (usually between 0.3 T and 1 T). Hence, it is justified to make an expansion with respect to  $\mathcal{F}^{-1} \Xi$ . For this, we apply the logarithm and use the expansion  $\log(1+x) \simeq x$  (for operators) together with the identity  $\log \det A = \text{Tr} \log A$ . Doing so, we obtain

$$\begin{aligned}
\sum_{i=1}^{\mathcal{N}} \log \varpi_i^2 &\simeq \sum_{i=1}^{\mathcal{N}} \log (\varpi_i^{(0)})^2 + \text{Tr} [\mathcal{F}^{-1} \Xi] \\
&= 2\mathcal{N} \log \varpi^{(0)} + \text{Tr} [\mathcal{F}^{-1} \Xi].
\end{aligned} \tag{26}$$

In order to compute the trace above, we only need to collect the (block) diagonals of the matrix  $\mathcal{F}^{-1} \Xi$  whose first block is as follows (showing only the diagonal elements)

$$\begin{aligned}
&\frac{1}{(\varpi^{(0)})^2} \begin{pmatrix} -F_{ii}^{\varphi\theta} & F_{ii}^{\theta\theta} \\ -F_{ii}^{\varphi\varphi} & F_{ii}^{\theta\varphi} \end{pmatrix} \begin{pmatrix} \Theta_{ii}^{\theta\varphi} & -\Theta_{ii}^{\theta\theta} \\ \Theta_{ii}^{\varphi\varphi} & -\Theta_{ii}^{\varphi\theta} \end{pmatrix} \\
&= \frac{1}{(\varpi^{(0)})^2} \begin{pmatrix} F_{ii}^{\theta\theta} \Theta_{ii}^{\varphi\varphi} - F_{ii}^{\varphi\theta} \Theta_{ii}^{\theta\theta} & * \\ * & F_{ii}^{\varphi\varphi} \Theta_{ii}^{\theta\theta} - F_{ii}^{\theta\varphi} \Theta_{ii}^{\varphi\theta} \end{pmatrix}
\end{aligned}$$

and thereby we obtain

$$\begin{aligned}
\text{Tr} [\mathcal{F}^{-1} \Xi] &= \frac{1}{(\varpi^{(0)})^2} \sum_{i=1}^{\mathcal{N}} [F_{ii}^{\theta\theta} \Theta_{ii}^{\varphi\varphi} \\
&\quad - (F_{ii}^{\varphi\theta} \Theta_{ii}^{\theta\varphi} + F_{ii}^{\theta\varphi} \Theta_{ii}^{\varphi\theta}) + F_{ii}^{\varphi\varphi} \Theta_{ii}^{\theta\theta}].
\end{aligned}$$

Thus, Eq. (26) becomes

$$\begin{aligned}
\frac{1}{\mathcal{N}} \sum_{i=1}^{\mathcal{N}} \log \varpi_i &= \log \varpi^{(0)} + \frac{1}{2\mathcal{N}(\varpi^{(0)})^2} \sum_{i=1}^{\mathcal{N}} [F_{ii}^{\theta\theta} \Theta_{ii}^{\varphi\varphi} \\
&\quad - (F_{ii}^{\varphi\theta} \Theta_{ii}^{\theta\varphi} + F_{ii}^{\theta\varphi} \Theta_{ii}^{\varphi\theta}) + F_{ii}^{\varphi\varphi} \Theta_{ii}^{\theta\theta}].
\end{aligned}$$

Next, it is quite reasonable to drop the sum on the left-hand side of the equation above as long as one considers nano-element arrays which are large enough and spatially isotropic. Then, upon expanding with respect to the small parameter  $\varpi_i/\varpi^{(0)} \lesssim 1$ , we obtain the final expression for the DI-induced frequency shift  $\Delta\varpi_{\text{DI}} \equiv \varpi - \varpi^{(0)}$

$$\begin{aligned}
\Delta\varpi_{\text{DI}} &\simeq \frac{1}{2\varpi^{(0)}} \frac{1}{\mathcal{N}} \sum_{i=1}^{\mathcal{N}} [F_{ii}^{\theta\theta} \Theta_{ii}^{\varphi\varphi} \\
&\quad - (F_{ii}^{\varphi\theta} \Theta_{ii}^{\theta\varphi} + F_{ii}^{\theta\varphi} \Theta_{ii}^{\varphi\theta}) + F_{ii}^{\varphi\varphi} \Theta_{ii}^{\theta\theta}].
\end{aligned} \tag{27}$$

We recall here again that the various matrix elements appearing above are second derivatives of the energy with respect to the system coordinates, evaluated at the equilibrium state  $\{\mathbf{s}^{(0)}\}$ , with  $\mathbf{s}^{(0)} = (1, 0, 0)$ . In some particular situations of anisotropy and field setup, the matrix  $\Xi$  can be explicitly computed, thus directly rendering the correction to the FMR frequency. Accordingly, in the next section we give explicit results for the specific case of nano-elements with effective uniaxial anisotropy along the field direction.

## C. FMR frequency of a 2D array of nanomagnets

### 1. DI-induced frequency shift

Now, we come to the evaluation of the matrix elements appearing in Eq. (27).

For the non-interacting case we have

$$F_{ii} = \begin{pmatrix} \partial_{\theta_i}^2 \mathcal{E}_i^{(0)} & \frac{1}{\sin \theta_i} \partial_{\theta_i \varphi_i}^2 \mathcal{E}_i^{(0)} \\ \frac{1}{\sin \theta_i} \partial_{\varphi_i \theta_i}^2 \mathcal{E}_i^{(0)} & \frac{1}{\sin^2 \theta_i} \partial_{\varphi_i}^2 \mathcal{E}_i^{(0)} \end{pmatrix} = \begin{pmatrix} \varpi^{(0)} & 0 \\ 0 & \varpi^{(0)} \end{pmatrix}.$$

For the DI contribution, both derivatives  $\partial_{\theta_i}^2 \mathcal{E}_{\text{DI}}$  and  $\partial_{\varphi_i}^2 \mathcal{E}_{\text{DI}}$  survive in Eq. (27) when evaluated at the equilibrium state ( $\theta_i = \pi/2, \varphi_i = 0$ ), whereas the cross derivatives vanish. Consequently, we obtain

$$\Theta_{ii}^{\theta\theta} = \Theta_{ii}^{\varphi\varphi} = - \left( \frac{\lambda}{2K_2V} \right) \sum_{\substack{j=1 \\ j \neq i}}^{\mathcal{N}} \frac{\mathcal{I}_d^h(\eta_{ij}, \tau)}{r_{ij}^3} \Phi_{ij}.$$

Next, using (13) and introducing the geometrical factor  $\kappa$  as the ratio of the inter-element separation  $d$  to their diameter  $D = 2R$ , *i.e.*  $\kappa = d/D$  [see Eq. (4)], we may rewrite the result above as follows

$$\Theta_{ii}^{\theta\theta} = \Theta_{ii}^{\varphi\varphi} = - \frac{A}{\kappa^3} \sum_{\substack{j=1 \\ j \neq i}}^{\mathcal{N}} \frac{\mathcal{J}_d^h(\eta_{ij}, \tau)}{r_{ij}^3}$$

where we have introduced the material-dependent constant

$$A \equiv \left( \frac{\mu_0}{4\pi} \right) \frac{m^2/D^3}{2K_2V} = \left( \frac{\mu_0}{8\pi} \right) \frac{M_s^2V}{K_2D^3}.$$

Then, substituting this result in Eq. (27) we arrive at the explicit DI correction to the FMR (dimensionless) angular frequency  $\varpi$  of the array of nano-magnets

$$\Delta\varpi_{\text{DI}} \simeq - \frac{A}{\kappa^3} \times \frac{1}{\mathcal{N}} \sum_{i=1}^{\mathcal{N}} \sum_{\substack{j=1 \\ j \neq i}}^{\mathcal{N}} \frac{\mathcal{J}_d^h(\eta_{ij}, \tau)}{r_{ij}^3}. \quad (28)$$

## 2. 2D array of nano-disks

The DI correction to the FMR frequency given in Eq. (28) is an implicit expression that depends on various parameters pertaining both to the nano-elements themselves (size, shape, energy) and to the assembly (spatial arrangement and shape). In particular, the nano-elements separation  $d$  enters this expression via the integral  $\mathcal{J}_d^h(\eta_{ij}, \tau)$  and the parameter  $\kappa$ . In order to derive an explicit (analytical) expression for the frequency shift in terms of the nano-elements separation  $d$  (or the parameter  $\kappa$ ), one has to (numerically) compute the integrals  $\mathcal{I}_d^h(\eta, \tau)$  and  $\mathcal{J}_d^h(\eta, \tau)$ . However, this can also be analytically done in some limiting cases of the parameters  $\eta$  and  $\tau$ , namely  $\tau \ll 1$  for thin disks (or platelets) or  $\tau \gg 1$  for long cylinders (or wires). By way of illustration, in the

present work we perform these calculations in the case of thin disks.

For thin disks ( $\tau \ll 1$ ), the integrands in Eq. (14) decay to zero for  $q \gtrsim 3$ . Hence, we can expand the exponential in these integrals up to the first order and then expand the integrals in powers of  $1/\kappa$  (for  $\kappa > 1$ ). This yields

$$\begin{aligned} \mathcal{J}_d^h(\kappa_{ij}, \tau) &\simeq 1 + \frac{9}{16\kappa^2} \times \frac{1}{r_{ij}^2}, \\ \mathcal{I}_d^h(\kappa_{ij}, \tau) &\simeq 1 + \frac{3}{16\kappa^2} \times \frac{1}{r_{ij}^2}, \end{aligned} \quad (29)$$

and

$$\Phi(\kappa_{ij}, \tau) = \frac{\mathcal{J}_d^h(\kappa_{ij}, \tau)}{\mathcal{I}_d^h(\kappa_{ij}, \tau)} \simeq 1 + \frac{3}{8\kappa^2} \times \frac{1}{r_{ij}^2}. \quad (30)$$

To be specific, we consider the FeV disks of Ref. 38 with  $D = 600$  nm,  $L = 26.7$  nm and a center-to-center separation  $d = 1600$  nm, we have  $\tau = 1/(2\delta) = L/D = 0.0445$ ,  $\eta = d/L \simeq 60$  and thereby  $\kappa = \eta\tau = d/D = 2.667$ . Therefore, the condition for the validity of the results above, *i.e.*  $\kappa > 1$  is satisfied even in the most unfavorable case.

Consequently, we obtain the frequency shift

$$\Delta\varpi_{\text{DI}} \simeq - \frac{A}{\kappa^3} \left[ \mathcal{C}_3 + \frac{9}{16\kappa^2} \mathcal{C}_5 \right] \quad (31)$$

where we have introduced the lattice sum

$$\mathcal{C}_n \equiv \frac{1}{\mathcal{N}} \sum_{i=1}^{\mathcal{N}} \sum_{\substack{j=1 \\ j \neq i}}^{\mathcal{N}} \frac{1}{r_{ij}^n}.$$

We thus have to evaluate two lattice sums, the well-known one<sup>39</sup>  $\mathcal{C}_3 \equiv \sum_i \sum_{k, k \neq i} [1/(\mathcal{N}r_{ik}^3)]$ , which is equal to  $\mathcal{C}_3 \simeq 9$  and the other  $\mathcal{C}_5 \equiv \sum_i \sum_{k, k \neq i} [1/(\mathcal{N}r_{ik}^5)]$ , equal to  $\mathcal{C}_5 \simeq 5.1$ , both in the thermodynamic limit.

We may then rewrite Eq. (31) as follows (assuming  $\mathcal{C}_3 \neq 0$ , *i.e.* excluding spheres and cubes)

$$\Delta\varpi_{\text{DI}} \simeq \Delta\varpi_{\text{pda}} \left( 1 + \frac{9}{16\kappa^2} \frac{\mathcal{C}_5}{\mathcal{C}_3} \right) \quad (32)$$

where we have singled out the contribution  $\Delta\varpi_{\text{pda}} \equiv - (A/\kappa^3) \mathcal{C}_3$  that obtains within the PDA. As such, we see more explicitly the correction to the FMR frequency due to the size and shape of the nanomagnets. Both contributions in Eq. (32) are in the form of a dipolar-like term multiplied by a lattice sum. While the PDA term  $\Delta\varpi_{\text{pda}}$  scales with the nano-elements separation  $d$  as  $1/d^3$ , the term that stems from size and shape effects scales with  $d$  as  $1/d^5$ . The power 5 here arises from the

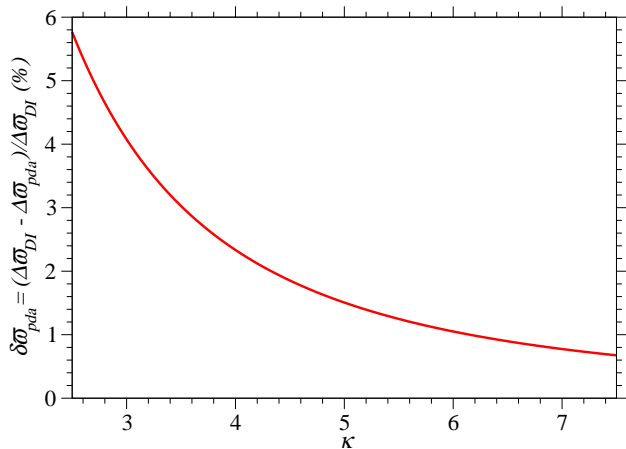


Figure 2: Relative variation of the frequency shift between PDA and cylindrical nanomagnets  $\delta\varpi_{\text{pda}} = \frac{|\Delta\varpi_{\text{DI}} - \Delta\varpi_{\text{pda}}|}{\Delta\varpi_{\text{DI}}}$  as a function of the distance  $\kappa$ .

3-dimensional space coordinates of the individual nanoparticles, plus the 2 space dimensions arising from the shape of the disks, for which the thickness is ignored (in the current thin-disk approximation). Likewise, the expansions of the shape integrals (29) and (30) also exhibit a point-dipole contribution together with a 2-dimensional shape correction that scales as  $1/\kappa^2$ . In Fig. 2 we plot the relative difference between  $\Delta\varpi_{\text{DI}}$  and  $\Delta\varpi_{\text{pda}}$ , namely  $\delta\varpi_{\text{pda}} = \frac{|\Delta\varpi_{\text{DI}} - \Delta\varpi_{\text{pda}}|}{\Delta\varpi_{\text{DI}}}$ . The results confirm that, for not-too-dense assemblies, *i.e.* for  $2.5 \lesssim \kappa \lesssim 3$ , there is a variation ( $\delta\varpi_{\text{pda}} \simeq 5\%$ ) of the frequency shift due to the fact that the nanomagnets are not simple point dipoles. This variation should be accessible to experiments. Obviously, for very dilute assemblies ( $\kappa \gtrsim 7$ ) the PDA provides a correct description of the physics up to an error less than 1%.

### III. SURFACE EFFECTS

In this section we discuss the impact of surface effects on the results obtained above. In an assembly of nanomagnets the intrinsic features of the latter, such as surface anisotropy (SA), are generally smoothed out by the distributions of size and (easy axis) orientation. However, in some situations, *e.g.* of monodisperse assemblies with oriented anisotropy, as is considered here, SE may lead to a non negligible contribution to the magnetic properties of the nano-elements, especially FMR frequency. Many examples of such assemblies have been fabricated by several experimental groups around the world, see the already cited works in the introduction as well Refs. 26,29,30,40. Surface effects are local effects whose study requires recourse to an atomic approach that accounts for the local atomic environment. However, from the computational point of view, taking account of such effects in an interacting assembly leads to tremendous difficulties

which cannot be efficiently dealt with even with the help of optimized numerical approaches. Nonetheless, in the limiting case of not-too-strong surface effects, inasmuch as the spin configuration inside of the nanomagnet can be regarded as quasi-collinear, the static and dynamic properties of the nanomagnet may be recovered with the help of an effective macroscopic model for the net magnetic moment of the nanomagnet. More precisely, it has been shown that a many-spin nanomagnet of a given lattice structure and energy parameters (on-site core and surface anisotropy, local exchange interactions) may be modeled by a macroscopic magnetic moment  $\mathbf{m}$  evolving in an effective potential<sup>20</sup>. The latter is, in principle an infinite polynomial in the components of  $\mathbf{m}$ , but whose leading terms are of two types, one is a quadratic and the other a quartic contribution with coefficients  $K_2$  and  $K_4$  that strongly depends on the microscopic parameters, as well as on the shape and size of the nanomagnet. Here, we would like to emphasize in passing the fact that the quartic term is a pure surface contribution, that appears even in the absence of core anisotropy [see Ref. 20,21] and which may renormalize the cubic anisotropy of the (underlying) magnetic material the nanomagnet is made of. However, there remains the question as to how one can distinguish this surface-induced fourth-order contribution from the (usually weak) cubic anisotropy found in magnetic materials. At least for thin disks where the effective anisotropy is mostly of (boundary) surface origin, this quartic contribution may become dominant. An example of this situation was provided by cobalt nano-dots with enhanced edge magnetic anisotropy<sup>41</sup>.

In the present work, we assume that the uniaxial anisotropy in Eq. (6), with coefficient  $K_2$ , is an effective anisotropy that already includes the (small) renormalization effect from surface anisotropy. On the other hand, the strongest contribution induced by surface effects is given by

$$E_i^{(\text{SE})} = \frac{1}{2}K_4 \sum_{\alpha=x,y,z} s_{i,\alpha}^4. \quad (33)$$

where  $K_4$  is a constant that scales with the square of the surface anisotropy constant<sup>20</sup>.  $K_4$  may be positive or negative, depending on the underlying magnetic material<sup>19</sup>. In the sequel, we will use the more relevant parameter  $\zeta \equiv K_4/K_2$ . Consequently, adding this contribution to the free-particle energy (6) adds the term  $-\zeta \sum_{\alpha=x,y,z} m_{i,\alpha}^3 e_\alpha$  to the effective field (10) and thereby the angular frequency of an isolated nanomagnet becomes  $\omega^{(0)} = \omega_K (h + k + h_d - \zeta)$ . Likewise, the corresponding dimensionless angular frequency is now given by  $\tilde{\omega}^{(0)} = h + k + h_d - \zeta \equiv \varpi^{(0)} + \varpi_{\text{SE}}$  [see Eq. (11)]. We see that due to the surface anisotropy contribution, the FMR frequency of a single nanomagnet may either increase or decrease according to the sign of  $\zeta$ . In particular, it is interesting to investigate how surface effects may make up for the frequency red-shift induced by dipolar interactions, as discussed earlier. Accordingly, the total frequency shift, due to both DI and surface effects, is

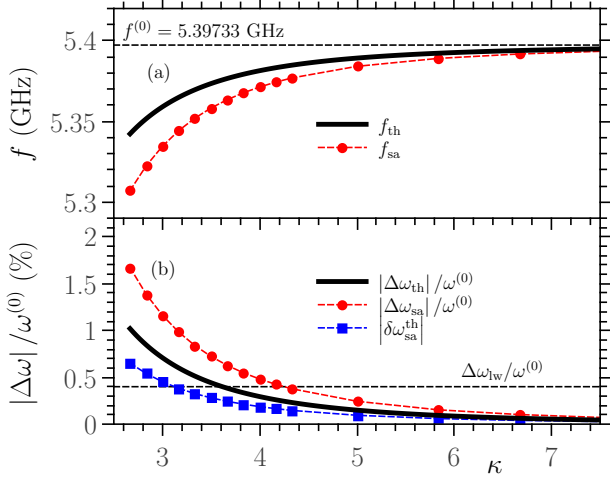


Figure 3: (a) Resonance frequency of an interacting  $20 \times 20$  square array of FeV nanodisks as a function of the relative nano-disk separation  $\kappa$ . The solid black line represents  $f_{th} = (\omega^{(0)} + \Delta\omega) / (2\pi)$ , where the frequency shift is obtained from Eq. (28). In red circles we present the semi-analytical uniform mode, obtained from the model of Ref. 42. Horizontal dashed line represents the resonance frequency in the non-interacting case. (b) Relative variation of the frequency shifts  $\Delta\omega_{th}/\omega^{(0)}$  and  $\Delta\omega_{sa}/\omega^{(0)}$  obtained from theory and semi-analytical calculations, respectively.  $\delta\omega_{sa}^{th}$  is the difference between the two approaches.

given by [see Eq. (31)]

$$\Delta\varpi = -\varpi_{SE} + \Delta\varpi_{DI} = \zeta - \frac{A}{\kappa^3} \left[ C_3 + \frac{9}{16\kappa^2} C_5 \right]. \quad (34)$$

For instance, for  $\zeta > 0$  we see that surface anisotropy may compete with dipolar interactions. This will be discussed in Section IV B.

#### IV. RESULTS AND DISCUSSION

Let us now discuss some of the results that can be inferred from Eq. (31) for the effect of DI and Eq. (34) when SE are included, especially in what regards the dependence of the shift in frequency on the parameter  $\kappa$ , that is the ratio of the nano-elements separation  $d$  to their diameter  $D$ .

##### A. Effects of dipolar interactions (ignoring surface effects)

For an order of magnitude and a comparison with other theoretical models, we consider for instance the ferromagnetic resonance of a finite  $20 \times 20$  square array. We compare the results from Eq. (28) with  $C_3 = 7.50253$  (for a square  $20 \times 20$  array) and those from the semi-analytical

model developed in Ref. 42 for multiple interacting magnetic moments. The dynamical fields arising from the dipolar coupling, which are necessary for calculating the FMR spectra of the nanoparticle array using the semi-analytical model, are given in Appendix B.

For the FeV disks, the thin-disk regime ( $L/(2R) \ll 1$ ) applies and thereby the frequency shift can be calculated using Eq. (31). The materials parameters are<sup>27,38</sup>:  $M_s = 1.353 \times 10^6$  A/m,  $H = 1.72$  T,  $K_v = 4.1 \times 10^4$  J/m<sup>3</sup>, and from Eq. (9) we can infer  $H_K \simeq 0.0606$  T and  $\omega_K = \gamma H_K \simeq 10.67 \times 10^9$  rad.s<sup>-1</sup>. Next, from Fig. 3(c) of Ref. 38 we can read off the frequency of the isolated elements,  $f^{(0)} \simeq 5.35$  GHz or  $\omega_{exp}^{(0)} \simeq 33.62 \times 10^9$  rad.s<sup>-1</sup>. We can also compute the effective field using Eq. (10).  $\delta = R/L \simeq 11.24$  leading to  $N_x = 0.956$ ,  $N_z = 0.022$  and  $H_d \simeq -1.59$  T. Note that for an infinitely thin disk ( $N_x \rightarrow 1$  and  $N_z \rightarrow 0$ ) we would obtain  $|H_d| \simeq 1.7$  T. Then, since  $H > |H_d|$  we may consider the magnetic moment of the disks to be aligned along the direction of the applied magnetic field, *i.e.*  $s_x \simeq 1$  and thereby the effective field evaluates to  $H_{eff} \simeq 0.193$  T. This yields the (theoretical) frequency of non-interacting nano-elements  $\omega_{th}^{(0)} = \gamma H_{eff} \simeq 33.91 \times 10^9$  rad.s<sup>-1</sup>, which is in good agreement with the experimental value  $\omega_{exp}^{(0)}$ .

Now, regarding the comparison between our work and the experiments of Ref. 38, beyond the agreement of the orders of magnitude, an important warning is necessary. In Fig. 4 of this reference, the authors plot the difference in frequency between the anti-binding and binding modes as a function of the nano-elements separation. Apart from the fact that only 3 values of the latter were available, and despite the (apparent) qualitative agreement with our theory, it is not possible to compare these experiments with our theory. Indeed, as discussed earlier, our approach only renders the frequency of the collective mode, which is here the binding mode, and it is not possible to derive the frequency of the anti-binding mode as this would require the full solution of the eigenvalue problem. On the other hand, the individual frequencies of the two modes cannot be extracted from these experiments because the nano-disks are not fully identical and their distances to the sensor are not equal either.

In Fig. 3(a) we plot the resonance frequency obtained from Eq. (31) ( $f_{th} = [\omega^{(0)} + \Delta\omega] / (2\pi)$  - black solid line) as a function of the relative distance parameter  $\kappa$ , together with the frequency ( $f_{sa}$ ) of the uniform resonance mode of the system obtained from the semi-analytical model<sup>42</sup> (red dashed line with circles). As expected, the dipolar coupling reduces the frequency relative to the non-interacting case (horizontal dashed line). The shift decreases as the distance between the disks increases, which is equivalent to a decrease in the dipolar coupling. Both theoretical calculations render the same qualitative behavior, with some quantitative discrepancies, especially for stronger DI. This is due to the several approximations and expansions used in the derivation of Eq. (31). Nonetheless, we can clearly see that the differ-

ence is reduced as  $\kappa$  increases, reaching a good agreement for  $\kappa \geq 5$ .

Fig. 3(b), shows the variation of the relative frequency shift  $|\Delta\omega|/\omega^{(0)}$  of each approach, and the difference  $\delta\omega_{\text{sa}}^{\text{sh}} \equiv (\Delta\omega_{\text{th}} - \Delta\omega_{\text{sa}})/\omega^{(0)}$ .  $\Delta\omega_{\text{th}}$  and  $\Delta\omega_{\text{sa}}$  are the absolute frequency shifts induced by the dipolar coupling, obtained from Eq. (31) and the semi-analytical model, respectively. We see that the DI induce small frequency shifts on the order of 1.5 % or even lower for the explored distances. Furthermore, we can see that when Eq. (31) becomes a good approximation ( $\kappa \geq 5$ ), the relative frequency shifts are on the order of 0.3 %. This relative variation expressed as a percentage is below typical relative experimental linewidths in similar systems (linewidth  $\Delta\omega_{\text{lw}}/(2\pi) \simeq 20$  MHz,  $\omega^{(0)}/(2\pi) \simeq 5$  GHz<sup>38</sup>, thus  $\Delta\omega_{\text{lw}}/\omega^{(0)} = 0.4$  %). However, increasing  $\omega^{(0)}$  (e.g. by increasing the applied field) reduces the relative frequency shift  $|\Delta\omega|/\omega^{(0)}$  and the error  $\delta\omega_{\text{sa}}^{\text{sh}}$ . As a consequence, the validity of our formalism [see Eq. (31)] extends to stronger interactions (smaller  $\kappa$ ), making it possible to reach the regime where the predicted frequency shifts can be measured in experiments.

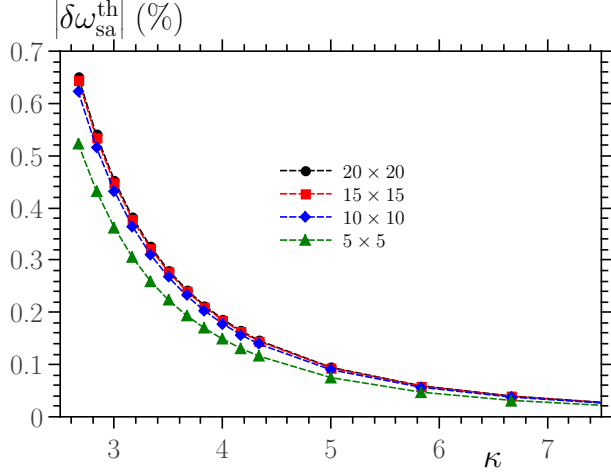


Figure 4: Error in the relative shift in frequency as a function of the relative distance  $\kappa$  for different sizes of a square array of disks.

The dependence of  $\delta\omega_{\text{sa}}^{\text{th}}$  on  $\kappa$  for different sizes of the array is shown in Fig. 4. It can be clearly seen that the error decreases for smaller arrays. Indeed, decreasing the size of the array decreases the overall dipolar contributions, thus making the different approximations more precise. Furthermore, it can also be seen that the error tends to stabilize as the size of the array increases, and no important variations are expected for arrays larger than  $20 \times 20$ .

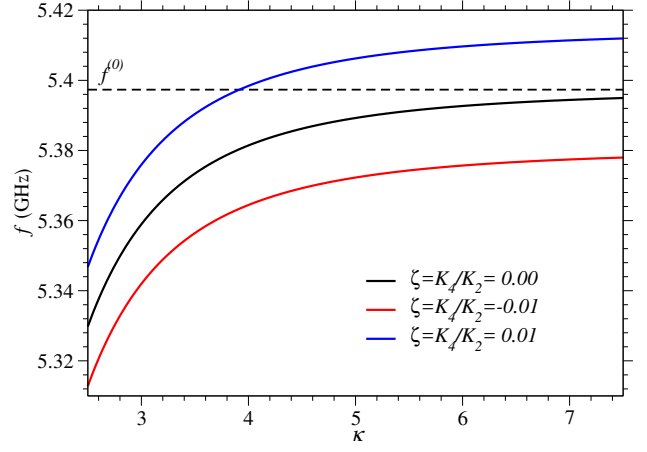


Figure 5: FMR frequency as a function of the relative nanodisk distance  $\kappa$  for various surface anisotropies  $\zeta = K_4/K_2$ .

### B. Effects of dipolar interactions including surface effects

Eq. (34) clearly reveals a competition between the effects of surface anisotropy and DI on the FMR frequency. In order to better assess the role of SE, we consider an interacting  $20 \times 20$  array of nano-disks similar to the sample of Fig. 3. The results are shown in Fig. 5 where we have restricted our investigation to the case of small surface anisotropy *i.e.*  $|\zeta| \ll 1$  in order to remain within the limits of the effective macrospin model [see discussion in Section III]<sup>18,19</sup>. First, analyzing the effect of surface anisotropy alone, we see that changing the value and sign of  $\zeta$  has a large effect on the FMR frequency, taking  $f^{(0)}$  as a reference. Now, for 2D square arrays the dipolar interactions tend to maintain the magnetic moments within the plane. In contrast, depending on the sign of  $\zeta$ , SE favor a magnetic alignment along the cube facets ( $\zeta < 0$ ), or along the cube diagonals ( $\zeta > 0$ ). Therefore, for materials with  $\zeta > 0$  one may expect a competition between SE and DI. This is what is observed in Fig. 5: at high densities (small  $\kappa$ ) DI dominate the correction to the FMR frequency and induce a red-shift, whereas for very dilute assemblies (large  $\kappa$ ) each nanodisk behaves like an isolated entity and SE dominate<sup>30</sup> and induce a blue-shift. At leading orders in  $\kappa$ , the critical value  $\kappa_c$  marking the crossover from a red- to a blue-shift is given by  $\kappa_c \simeq (AC_3/\zeta)^{1/3}$ . This is the point where the blue line crosses the dashed line in Fig. 5, implying that SE compensate for the DI. For the FeV thin disks considered here,  $\kappa_c \simeq 3.9$ . This corresponds to an inter-element separation of 4 times the element diameter, *i.e.* a center-to-center distance of 2400 nm.

The value of  $\zeta$  taken here is rather small as compared to the estimates obtained by other authors in cobalt and iron-oxide elements<sup>15–17</sup>. For such higher values (an order of magnitude larger) of surface anisotropy, compensation of the DI effects should occur for much closer nano-

elements, or equivalently denser assemblies. However, this reasoning cannot be taken too far, at least in the framework of our approach, since our treatment is limited to dilute assemblies and not-too-strong surface disorder. Nonetheless, it does confirm the screening effect of DI by surface disorder studied earlier by the authors<sup>43,44</sup>.

## V. CONCLUSION

We have developed a general formalism for deriving practical analytical formulas for the shift in FMR frequency induced by both dipolar interactions and surface disorder in an array of magnetic nano-elements. Even though this has been done with the help of perturbation theory, which only applies to relatively dilute assemblies, or equivalently for well separated nano-elements, the general character of this formalism resides in the fact that it applies to nano-elements of arbitrary shape and size, and as such, it deals with the dipolar interactions beyond the point-dipole approximation. An analytical expression for the frequency shift induced by dipolar interactions has been explicitly derived for an arbitrary array of monodisperse elements, and the contribution due to their shape and size has been singled out. Next, this formalism has been applied to the limiting case of thin disks of FeV, recently investigated by the technique of Magnetic Resonance Force Microscopy. We have clearly shown that the contribution of dipolar interactions to the FMR frequency of a  $2D$  array of nano-elements is a linear function of the parameter  $\xi$  which scales as the inverse of the third power of the elements separation. In addition to this contribution, that obtains within the point-dipole approximation, we also obtain a contribution from the nano-elements size and shape which scales with the inverse fifth power of the nano-elements separation. We have also studied the effect of the array size on the frequency shift and have found that the red-shift of the resonance is smaller for smaller arrays. The effects of surface anisotropy on the frequency shift have been taken into account with the help of an effective macroscopic model for the isolated nano-elements. Depending on the sign of the corresponding contribution, which changes with the properties pertaining to the nano-element itself, we may obtain either a blue-shift or a red-shift of the FMR frequency. Correspondingly, this may lead to a competition or a concomitant effect with the dipolar interactions. This means that surface anisotropy and dipolar interactions provide us with a handle for adjusting the resonance frequency of nano-magnet assemblies.

### Acknowledgments

A. F. Franco acknowledges financial support from the FONDECYT postdoctoral project No 3150180.

## Appendix A: The pseudo-Hessian matrix elements for the DI contribution

The following general expressions<sup>37</sup> are used in the calculation of the second derivatives of the DI contribution with respect to the angular variables  $(\theta_i, \varphi_i)$

$$\begin{aligned} \partial_{\theta_i \theta_k}^2 \mathcal{E}_{\text{DI}} &= -\delta_{ik} \sum_{j=1}^{\mathcal{N}} \xi_{ij} (1 - \delta_{ij}) \mathbf{s}_i \cdot \mathcal{D}_{ij} \cdot \mathbf{s}_j \quad (\text{A1}) \\ &\quad + \xi_{ik} (1 - \delta_{ik}) (\mathbf{e}_{\theta_i} \cdot \mathcal{D}_{ik} \cdot \mathbf{e}_{\theta_k}) \\ \partial_{\varphi_i \varphi_k}^2 \mathcal{E}_{\text{DI}} &= -\delta_{ik} \sum_{j=1}^{\mathcal{N}} \xi_{ij} (1 - \delta_{ij}) \times \\ &\quad [(\sin^2 \theta_i \mathbf{s}_i + \sin \theta_i \cos \theta_i \mathbf{e}_{\theta_i}) \cdot \mathcal{D}_{ij} \cdot \mathbf{s}_j] \\ &\quad + \xi_{ik} (1 - \delta_{ik}) \sin \theta_i \sin \theta_k (\mathbf{e}_{\varphi_i} \cdot \mathcal{D}_{ik} \cdot \mathbf{e}_{\varphi_k}) \\ \partial_{\theta_k \varphi_i}^2 \mathcal{E}_{\text{DI}} &= \delta_{ik} \sum_{j=1}^{\mathcal{N}} \xi_{ij} (1 - \delta_{ij}) \cos \theta_i (\mathbf{e}_{\varphi_i} \cdot \mathcal{D}_{ij} \cdot \mathbf{s}_j) \\ &\quad + \xi_{ik} (1 - \delta_{ik}) \sin \theta_i (\mathbf{e}_{\varphi_i} \cdot \mathcal{D}_{ik} \cdot \mathbf{e}_{\theta_k}) \\ \partial_{\varphi_k \theta_i}^2 \mathcal{E}_{\text{DI}} &= \delta_{ik} \sum_{j=1}^{\mathcal{N}} \xi_{ij} (1 - \delta_{ij}) \cos \theta_i (\mathbf{e}_{\varphi_i} \cdot \mathcal{D}_{ij} \cdot \mathbf{s}_j) \\ &\quad + \xi_{ik} (1 - \delta_{ik}) \sin \theta_k (\mathbf{e}_{\theta_i} \cdot \mathcal{D}_{ik} \cdot \mathbf{e}_{\varphi_k}), \end{aligned}$$

with

$$\begin{aligned} \mathbf{e}_{\theta_i} &= \partial_{\theta_i} \mathbf{s}_i = \begin{pmatrix} \cos \theta_i \cos \varphi_i \\ \cos \theta_i \sin \varphi_i \\ -\sin \theta_i \end{pmatrix}, \\ \mathbf{e}_{\varphi_i} &= \frac{1}{\sin \theta_i} \partial_{\varphi_i} \mathbf{s}_i = \begin{pmatrix} -\sin \varphi_i \\ \cos \varphi_i \\ 0 \end{pmatrix}. \end{aligned}$$

## Appendix B: Dynamical dipolar fields

The dynamical fields due to the dipolar coupling can be calculated in the context of the model presented in<sup>42</sup> for the propagation of in-plane spin waves in multilayer systems. This model can be applied to the array of interacting nano-particles presented here for the zero wave-vector (uniform mode). Starting from Eq. (12) (in SI units), and following a similar procedure as the one presented in<sup>42</sup>, the following dipolar dynamical fields were obtained

with  $\varphi_{i,j}^{\pm} \equiv \varphi_i \pm \varphi_j$ .

$$\begin{aligned}
H_{x_i x_i}^d &= - \sum_{j \neq i} \frac{M_s^j}{4\pi r_{ij}^3} [\Phi_{ij} \cos \theta_i \cos \theta_j + \sin \theta_i \sin \theta_j \\
&\quad \times (\cos \varphi_{i,j}^- - (2 + \Phi_{ij}) (r_{ij,x} r_{ij,y} \sin \varphi_{i,j}^+ \\
&\quad + r_{ij,x}^2 \cos \varphi_i \cos \varphi_j + r_{ij,y}^2 \sin \varphi_i \sin \varphi_j))] \\
H_{y_i y_i}^d &= H_{x_i x_i}^d \\
H_{x_i x_j}^d &= \frac{M_s^j}{4\pi r_{ij}^3} [\Phi_{ij} \sin \theta_i \sin \theta_j + \cos \theta_i \cos \theta_j \\
&\quad \times (\cos \varphi_{i,j}^- - (2 + \Phi_{ij}) (r_{ij,x} r_{ij,y} \sin \varphi_{i,j}^+ \\
&\quad + r_{ij,x}^2 \cos \varphi_i \cos \varphi_j + r_{ij,y}^2 \sin \varphi_i \sin \varphi_j))] \\
H_{y_i y_j}^d &= \frac{M_s^j}{4\pi r_{ij}^3} [\cos \varphi_{i,j}^- - (2 + \Phi_{ij}) (r_{ij,x}^2 \sin \varphi_i \sin \varphi_j \\
&\quad + r_{ij,y}^2 \cos \varphi_i \cos \varphi_j - r_{ij,x} r_{ij,y} \sin \varphi_{i,j}^-)] \\
H_{x_i y_j}^d &= \frac{M_s^j}{4\pi r_{ij}^3} \cos \theta_i [\sin \varphi_{i,j}^- + (2 + \Phi_{ij}) \\
&\quad \times (r_{ij,x}^2 \cos \varphi_i \sin \varphi_j - r_{ij,y}^2 \sin \varphi_i \cos \varphi_j \\
&\quad - r_{ij,x} r_{ij,y} \cos \varphi_{i,j}^+)] \\
H_{y_i x_j}^d &= - \frac{M_s^j}{4\pi r_{ij}^3} \cos \theta_j [\sin \varphi_{i,j}^- - (2 + \Phi_{ij}) \\
&\quad \times (r_{ij,x}^2 \sin \varphi_i \cos \varphi_j - r_{ij,y}^2 \cos \varphi_i \sin \varphi_j \\
&\quad - r_{ij,x} r_{ij,y} \cos \varphi_{i,j}^+)] ,
\end{aligned}$$

\* Electronic address: [dejardin@univ-perp.fr](mailto:dejardin@univ-perp.fr)

† Electronic address: [andres.franco@usm.cl](mailto:andres.franco@usm.cl)

‡ Electronic address: [francois.vernay@univ-perp.fr](mailto:francois.vernay@univ-perp.fr)

§ Electronic address: [hamid.kachkachi@univ-perp.fr](mailto:hamid.kachkachi@univ-perp.fr)

<sup>1</sup> S. V. Vonsovskii, *Ferromagnetic Resonance: The Phenomenon of Resonant Absorption of a High-Frequency Magnetic Field in Ferromagnetic Substances* (Pergamon Press, Oxford, 1966).

<sup>2</sup> A.G. Gurevich and G.A. Melkov, *Magnetization oscillations and waves* (CSC Press, Florida, 1996).

<sup>3</sup> M. Tran, Master's thesis, Institut National des Sciences Appliquees de Toulouse, Toulouse (2006).

<sup>4</sup> B. Heinrich, in *Ultrathin magnetic structures II*, edited by B. Heinrich and J. Bland (Springer-Verlag, Berlin, 1994), p. 195.

<sup>5</sup> J. S. Lee, R. P. Tan, J. H. Wu, and Y. K. Kim, *Appl. Phys. Lett.* **99**, 062506 (2011), <https://doi.org/10.1063/1.3624833>, URL <https://doi.org/10.1063/1.3624833>.

<sup>6</sup> A. M. Gonçalves, I. Barsukov, Y.-J. Chen, L. Yang, J. A. Katine, and I. N. Krivorotov, *Applied Physics Letters* **103**, 172406 (2013), <https://doi.org/10.1063/1.4826927>, URL <https://doi.org/10.1063/1.4826927>.

<sup>7</sup> C. Schoepner, K. Wagner, S. Stienen, R. Meckenstock, M. Farle, R. Narkowicz, D. Suter, and J. Lindner, *Journal of Applied Physics* **116**, 033913 (2014), <https://doi.org/10.1063/1.4890515>, URL <https://doi.org/10.1063/1.4890515>.

<sup>8</sup> K. Ollefs, R. Meckenstock, D. Spoddig, F. M. Römer, C. Hassel, C. Schöppner, V. Ney, M. Farle, and A. Ney, *Journal of Applied Physics* **117**, 223906 (2015), <https://doi.org/10.1063/1.4922248>, URL <https://doi.org/10.1063/1.4922248>.

<sup>9</sup> J. A. Sidles, J. L. Garbini, K. J. Bruland, D. Rugar, O. Züger, S. Hoen, and C. S. Yannoni, *Rev. Mod. Phys.* **67**, 249 (1995), URL <http://link.aps.org/doi/10.1103/RevModPhys.67.249>.

<sup>10</sup> Lavenant, H., Naletov, V. V. Klein, O. De Loubens, G. Laura, C. De Teresa, J. M., *Nanofabrication* **1**, 65 (2014).

<sup>11</sup> C. Kittel, *Phys. Rev.* **73**, 155 (1948), URL <https://link.aps.org/doi/10.1103/PhysRev.73.155>.

<sup>12</sup> G. J. Strijkers, J. H. J. Dalderop, M. A. A. Broeksteeg, H. J. M. Swagten, and W. J. M. de Jonge, *Journal of Applied Physics* **86**, 5141 (1999), URL <http://scitation.aip.org/content/aip/journal/jap/86/9/10.1063/1.371490>.

<sup>13</sup> A. Encinas-Oropesa, M. Demand, L. Piroux, U. Ebels, and I. Huynen, *Journal of Applied Physics* **89**, 6704 (2001), <https://doi.org/10.1063/1.1362638>, URL <https://doi.org/10.1063/1.1362638>.

<sup>14</sup> H. T. Yang, D. Hasegawa, M. Takahashi, and T. Ogawa, *Applied Physics Letters* **94**, 013103 (2009), <https://doi.org/10.1063/1.3063032>, URL <https://doi.org/10.1063/1.3063032>.

<sup>15</sup> K. B. Urquhart, B. Heinrich, J. F. Cochran, A. S. Arrott, and K. Myrtle, *Journal of Applied Physics* **64**, 5334

- (1988), <https://doi.org/10.1063/1.342362>, URL <https://doi.org/10.1063/1.342362>.
- 16 R. Skomski and J.M.D. Coey, *Permanent Magnetism, Studies in Condensed Matter Physics Vol. 1* (IOP Publishing, London, 1999).
  - 17 R. Perzynski and Yu.L. Raikher, in *Surface effects in magnetic nanoparticles*, edited by D. Fiorani (Springer, Berlin, 2005), p. 141.
  - 18 H. Kachkachi and E. Bonet, *Phys. Rev. B* **73**, 224402 (2006), URL <https://link.aps.org/doi/10.1103/PhysRevB.73.224402>.
  - 19 R. Yanes, O. Chubykalo-Fesenko, H. Kachkachi, D. A. Garanin, R. Evans, and R. W. Chantrell, *Phys. Rev. B* **76**, 064416 (2007), URL <https://link.aps.org/doi/10.1103/PhysRevB.76.064416>.
  - 20 D. A. Garanin and H. Kachkachi, *Phys. Rev. Lett.* **90**, 065504 (2003), URL <http://link.aps.org/doi/10.1103/PhysRevLett.90.065504>.
  - 21 H. Kachkachi, *Journal of Magnetism and Magnetic Materials* **316**, 248 (2007), ISSN 0304-8853, Proceedings of the Joint European Magnetic Symposia, URL <http://www.sciencedirect.com/science/article/pii/S0304885307005252>.
  - 22 R. Verba, G. Melkov, V. Tiberkevich, and A. Slavin, *Phys. Rev. B* **85**, 014427 (2012), URL <https://link.aps.org/doi/10.1103/PhysRevB.85.014427>.
  - 23 M. Beleggia, S. Tandon, Y. Zhu, and M. D. Graef, *Journal of Magnetism and Magnetic Materials* **278**, 270 (2004), ISSN 0304-8853, URL <http://www.sciencedirect.com/science/article/pii/S0304885304000186>.
  - 24 V. V. Naletov, G. de Loubens, G. Albuquerque, S. Borlenghi, V. Cros, G. Faini, J. Grollier, H. Hurdequint, N. Locatelli, B. Pigeau, et al., *Phys. Rev. B* **84**, 224423 (2011), URL <https://link.aps.org/doi/10.1103/PhysRevB.84.224423>.
  - 25 A. Sukhov, P. P. Horley, J. Berakdar, A. Terwey, R. Meckenstock, and M. Farle, *IEEE Transactions on Magnetics* **50**, 1 (2014), ISSN 0018-9464, URL <http://ieeexplore.ieee.org/stamp/stamp.jsp?tp=&arnumber=6828754&isnumber=6980152>.
  - 26 T. N. Shendruk, R. D. Desautels, B. W. Southern, and J. van Lierop, *Nanotechnology* **18**, 455704 (2007), URL <http://stacks.iop.org/0957-4484/18/i=45/a=455704>.
  - 27 K. Mitsuzuka, D. Lacour, M. Hehn, S. Andrieu, and F. Montaigne, *Applied Physics Letters* **100**, 192406 (2012), <https://doi.org/10.1063/1.4711219>, URL <https://doi.org/10.1063/1.4711219>.
  - 28 I. Lisiecki and S. Nakamae, *Journal of Physics: Conference Series* **521**, 012007 (2014), URL <http://stacks.iop.org/1742-6596/521/i=1/a=012007>.
  - 29 H. Khusruid, Z. N. Porshokouh, M.-H. Phan, P. Mukherjee, and H. Srikanth, *Journal of Applied Physics* **115**, 17E131 (2014), <https://doi.org/10.1063/1.4868619>, URL <https://doi.org/10.1063/1.4868619>.
  - 30 G. C. Lavorato, D. Peddis, E. Lima, H. E. Troiani, E. Agostinelli, D. Fiorani, R. D. Zysler, and E. L. Winkler, *The Journal of Physical Chemistry C* **119**, 15755 (2015), <https://doi.org/10.1021/acs.jpcc.5b04448>, URL <https://doi.org/10.1021/acs.jpcc.5b04448>.
  - 31 S. Tandon, M. Beleggia, Y. Zhu, and M. D. Graef, *Journal of Magnetism and Magnetic Materials* **271**, 9 (2004), ISSN 0304-8853, URL <http://www.sciencedirect.com/science/article/pii/S0304885303007467>.
  - 32 A. Caciagli, R. J. Baars, A. P. Philipse, and B. W. Kuipers, *Journal of Magnetism and Magnetic Materials* **456**, 423 (2018), ISSN 0304-8853, URL <http://www.sciencedirect.com/science/article/pii/S0304885317334662>.
  - 33 G. Wysin, *Demagnetization fields* (2012), URL <https://www.phys.ksu.edu/personal/wysin/notes/demag.pdf>.
  - 34 A. F. Franco, J. L. Déjardin, and H. Kachkachi, *Journal of Applied Physics* **116**, 243905 (2014), <https://doi.org/10.1063/1.4904750>, URL <https://doi.org/10.1063/1.4904750>.
  - 35 M. Varón, M. Beleggia, T. Kasama, R. Harrison, R. Dunin-Borkowski, V. Puntès, and C. Frandsen, *Scientific Reports* **3**, 1234 (2013), URL <http://dx.doi.org/10.1038/srep01234>.
  - 36 J. M. Luttinger and L. Tisza, *Phys. Rev.* **70**, 954 (1946), URL <https://link.aps.org/doi/10.1103/PhysRev.70.954>.
  - 37 R. Bastardis, F. Vernay, D.-A. Garanin, and H. Kachkachi, *Journal of Physics: Condensed Matter* **29**, 025801 (2017), URL <http://stacks.iop.org/0953-8984/29/i=2/a=025801>.
  - 38 B. Pigeau, C. Hahn, G. de Loubens, V. V. Naletov, O. Klein, K. Mitsuzuka, D. Lacour, M. Hehn, S. Andrieu, and F. Montaigne, *Phys. Rev. Lett.* **109**, 247602 (2012), URL <https://link.aps.org/doi/10.1103/PhysRevLett.109.247602>.
  - 39 P. E. Jönsson and J. L. García-Palacios, *Phys. Rev. B* **64**, 174416 (2001), URL <https://link.aps.org/doi/10.1103/PhysRevB.64.174416>.
  - 40 B. Issa, I. Obaidat, B. Albiss, and Y. Haik, *International Journal of Molecular Sciences* **14**, 21266 (2013), ISSN 1422-0067, URL <http://dx.doi.org/10.3390/ijms141121266>.
  - 41 S. Rohart, V. Repain, A. Thiaville, and S. Rousset, *Phys. Rev. B* **76**, 104401 (2007), URL <https://link.aps.org/doi/10.1103/PhysRevB.76.104401>.
  - 42 A. F. Franco and P. Landeros, *Journal of Physics D: Applied Physics* **49**, 385003 (2016), URL <http://stacks.iop.org/0022-3727/49/i=38/a=385003>.
  - 43 Z. Sabsabi, F. Vernay, O. Iglesias, and H. Kachkachi, *Phys. Rev. B* **88**, 104424 (2013), URL <https://link.aps.org/doi/10.1103/PhysRevB.88.104424>.
  - 44 F. Vernay, Z. Sabsabi, and H. Kachkachi, *Phys. Rev. B* **90**, 094416 (2014), URL <https://link.aps.org/doi/10.1103/PhysRevB.90.094416>.